

Optimization of computed tomography protocols based on objective and subjective evaluations.

**R.A.C. Guassu¹, S.A. Santana Souza¹, M. Alvarez², S.M. Ribeiro²,
J.C.S. Trindade Filho², D.R. Pina^{2*}**

¹Department of Physics and Biophysics, São Paulo State University Julio de Mesquita Filho, Institute of Bioscience, R. Prof. Dr. Antônio Celso Wagner Zanin, 250 - Distrito de Rubião Júnior, Botucatu, Brazil

²São Paulo State University Julio de Mesquita Filho, Medical School, Av. Prof. Mário Rubens Guimarães Montenegro - UNESP, Botucatu, Brazil

► Original article

***Corresponding author:**
Diana Rodrigues de Pina, Ph.D.,
E-mail: diana.pina@unesp.br

Received: November 2023

Final revised: April 2024

Accepted: June 2024

Int. J. Radiat. Res., April 2025;
23(2): 379-385

DOI: [10.61186/ijrr.23.2.17](https://doi.org/10.61186/ijrr.23.2.17)

Keywords: Computed tomography, dose optimization, image quality, thoracic imaging.

INTRODUCTION

Computed tomography has revolutionized medical image guidance, enabling precise target localization⁽¹⁾. Widely employed in medical imaging, it stands as a powerful diagnostic tool⁽²⁾. Although computed tomography has excellent medical diagnosis benefits, it can be associated with high ionizing radiation levels⁽¹⁻³⁾. Exposure to ionizing radiation during imaging can be responsible for cancer induction, causing 0.6-3.2% of malignant tumors in 15 developed countries^(4,5). Moreover, CT accounts for 70% of the radiation doses received in medical procedures⁽⁴⁾. In this context, the chest is one of the areas that receive the highest radiation dose in CT exams. This leads to a concern mainly because diseases like lung cancer have high mortality around the world⁽⁶⁾.

In recent years, the National Council on Radiation Protection and Measurements⁽⁷⁾ reported a significant increase in medical radiation exposure in the last 25 years. Medical exposure now essentially constitutes half of all radiation exposure for the U.S. population, primarily due to the increased utilization of computed tomography⁽⁸⁾.

Background: Computed tomography (CT) is a crucial technique in clinical practice for diagnosing thoracic pathologies. However, the risk associated with ionizing radiation requires measures to reduce patient exposure. **Materials and Methods:** This study aims to optimize thoracic CT protocols on a multislice CT scanner, using both objective and subjective analyses of image quality to decrease radiation dose without compromising diagnostic accuracy. A 16-channel CT scanner with automatic tube current modulation (ATCM) was utilized, along with an analytical phantom for objective evaluation. Six protocols with different standard deviation values were selected, including three used in clinical routines and three additional ones for testing. Parameters such as spatial resolution, low contrast resolution, noise, and dosimetry were assessed. Subjective Image Quality evaluation was conducted through visual grading analysis (VGA). **Results:** Optimized protocols were selected based on acceptable image quality and dose results. Data were statistically analyzed, demonstrating that optimized protocols showed a significant reduction in radiation dose while maintaining adequate diagnostic quality. **Conclusion:** This study contributes to clinical practice by adhering to the ALARA (As Low As Reasonably Achievable) principles of dose reduction, ensuring accurate and safe diagnoses in thoracic CT examinations.

ABSTRACT

Dose reduction measures are necessary following the ALARA principle, which seeks to perform low-dose radiation exams without compromising the medical diagnosis reliability⁽⁹⁾. Among all the dose reduction techniques used in CT, Automatic Tube Current Modulation (ATCM) stands out. ATCM automatically adjusts the tube current in the x-y plane (angular modulation) along the z-axis based on the patient's size. Modulation is based on regional attenuation profile and other parameters, such as tube tension and table speed⁽⁸⁾.

Many studies have evaluated ATCM in different equipment, patients, and protocols⁽⁹⁻¹¹⁾. Each manufacturer uses different terminology for ATCM, such as standard deviation (SD) or index noise⁽¹²⁾. The correct implementation of ATCM in clinical protocols determines the proper radiation dose level for the patient's size and for the image quality level⁽¹³⁾. Despite their efficiency in choosing the appropriate current for each region of the patient, the clinical applications of ATCM techniques vary widely among institutions, which illustrate the lack of effective protocols standardization⁽³⁾.

This study aimed to optimize chest computed tomography protocols based on subjective image

quality evaluations using visual grading analysis and objective dose levels analyses. Then this study intended to determine a standard image quality based on objective methods to transfer those protocols to other CT equipment. Different protocols were tested through ATCM variation to determine the best relation between image quality and radiation dose, respecting the ALARA principle. It is essential to optimize protocols and achieve the patient's best risk-benefit relation (9, 11, 14).

By integrating subjective and objective evaluations, this research introduces an innovative approach to optimizing chest computed tomography protocols. Through the establishment of a standard image quality model and the utilization of ATCM alongside adherence to the ALARA principle, our study seeks to strike a balance between image quality and radiation dose, thereby enhancing the safety and efficacy of clinical practice.

MATERIALS AND METHODS

To achieve the objective of this study, the steps showed in figure 1 were followed:

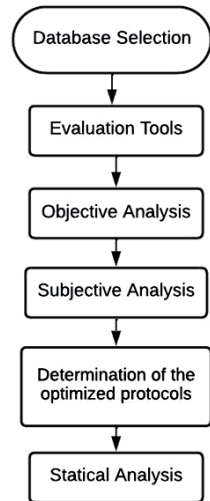


Figure 1. Flowchart illustrating the steps followed in the study to achieve the proposed objectives.

Database selection

All images used in this study were acquired with a 16-channel multislice computed tomography device, Toshiba Activion (Toshiba Medical Systems, Ottawa, Japan), with ATCM for CT images.

Thirty patients were included in the analysis. The inclusion criteria for these patients were body dimensions of about 75 kg weight and 1.75 m height [10]. Exclusion criteria were patients whose imaging protocols were acquired differently from the standard routine, or the ones who had pathologies that modified the lung parenchyma and rib cage.

CT protocol selection

In the optimization process, six protocols were evaluated, with three commonly used in clinical routine (protocols 1, 2, and 3) and three added for evaluation (protocols 4, 5, and 6). All protocols were

used for chest examinations of patients with various conditions, such as undefined pathologies, check-ups, neoplasms monitoring, metastases, and postoperative screening. The three routine protocols were selected based on the patient's anatomy.

Table 1 describes each protocol with different acquisition parameters, including kV and standard deviation (SD). A total of 30 patients were subjectively analyzed, with five patients selected for each protocol. The optimization process of the six protocols was based on: a) Dose levels estimative (Computed tomography dose index - CTDIvol, DLP - Dose length product, and Size-specific dose estimate - SSDE); and b) Subjective image analysis (Visual Grading Analysis - Subjective noise, Subjective spatial resolution, Diagnostic acceptability).

Table 1. Acquisition parameters of protocols for routine chest computed tomography exams for adults.

Protocol	1	2	3	4	5	6
Collimation (mm)	16×1.0	16×1.0	16×1.0	16×1.0	16×1.0	16×1.0
Slice thickness (mm)	5.0	5.0	5.0	5.0	5.0	5.0
Recon thickness (mm)	2.0	2.0	2.0	2.0	2.0	2.0
Pitch	1.125	1.125	1.125	1.125	1.125	1.125
Rotation time (s)	0.75	0.75	0.75	0.75	0.75	0.75
Tube voltage (kV)	120/100	120/100	120/100	120/100	120/100	120/100
Standard deviation	7.5	8.75	10	11.5	12	15

Evaluation tools

The American Association of Physicists in Medicine (AAPM) CT Performance Phantom was employed (model 610, computerized imaging reference systems, Inc., Virginia, USA) (15). This phantom consisted of three distinct sections designed to test different aspects of image quality, as depicted in figure 2.

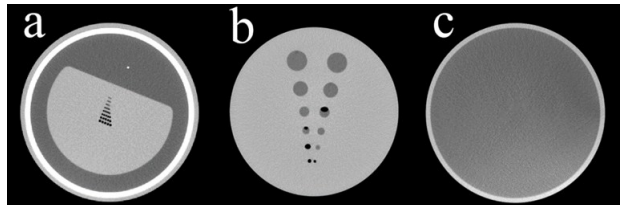


Figure 2. The objective evaluation of the image quality was performed using the AAPM CT Performance Phantom. It was used three different sections: (a) high-resolution section, (b) low contrast section, and (c) noise section.

a. Spatial resolution section: composed of groups of 8 holes in a Lucite block, ranging from 1.75 mm to 0.40 mm, with 4.3 mm longitudinal spacing, filled with air, as shown in figure 1 (12) for the analysis of Spatial Resolution.

b. Low contrast structures section: mounted at the end of the phantom tank, allows the user to evaluate

a scanner's ability to detect small differences in density, show in 1⁽¹⁶⁾. The cavities drilled in this section range from 1.0" OD to 0.365" OD. The acrylic block has a density of 1.19 gms/cm³. Solutions of dextrose or NaClH2O, prepared on a weight percent basis and differing by 1%, 2% or 3% from the acrylic density, were used to fill these cavities.

c. Noise Measurement section: A homogeneous section filled with water was used to evaluate image noise, as shown in figure 2⁽¹²⁾.

Objective Analysis

Dose levels analysis

According to the ALARA principle, dose levels should be as low as reasonably achievable. Therefore, a dose analysis was performed to determine an average dose in the patient. The reference dose levels were obtained in the European protocol⁽¹⁷⁾: Computed tomography dose index (CTDIvol<30mGy); Dose length product (DLP<650 mGycm); and Size-specific dose estimate (SSDE).

Image quality analysis

Image quality was assessed by evaluation of contrast-to-noise ratio (CNR); modulation transfer function (MTF); and Noise. These objective parameters were used to define the lower limits of image quality that will determine the minimum conditions for a chest protocol to have sufficient image quality for an acceptable medical report.

The levels of image quality for each protocol were determined. An objective evaluation through the AAPM phantom was performed, according to the following parameters:

I. Modulation transfer function (MTF) at 40%: The Modulation transfer function was used to assess the spatial resolution by using SD pixel values measurement within each cyclic hole pattern, in the first section of the AAPM CT Performance Phantom, following the methodology described in⁽¹⁸⁾.

II. Values of the contrast-to-noise ratio (CNR): The contrast-to-noise ratio was used to assess the low contrast in the second section of the AAPM CT Performance Phantom. It is defined as the signal difference between two adjacent areas, which directly determines the system's ability to distinguish them. It is characterized by equation 1⁽¹⁹⁾.

$$CNR = \frac{|S_A - S_B|}{\sigma_0} \quad (1)$$

SA and SB are the mean signal intensities (CT numbers) in Hounsfield units⁽²⁰⁾, and σ_0 was the SD in the background. Regions of Interest (ROIs) with 1.2 cm² were used. Area A was placed in each low contrast hole, while area B was placed in the background. This allowed the calculation of the CNR for each low contrast structure.

III. Noise levels: Noise was evaluated through the SD measured by circular ROIs at different points in the third section of the AAPM CT Performance

phantom.

Subjective analysis

The evaluation of the image quality through the assessment of radiologists followed the European Guidelines on Quality Criteria⁽¹⁷⁾.

Implementing the six protocols in the clinical routine was necessary to perform all evaluations. Afterwards, an analysis was carried out by two radiologists with more than 15 years of experience. They evaluated each protocol according to the following criteria:

Subjective noise - presence of noise that affects the image quality in general.

Subjective spatial resolution - visually sharp reproduction of the structures.

Diagnostic acceptability - how acceptable is the examination overall.

These parameters were classified by radiologists on a 5-point scale: +2: Great; +1 good quality; 0: acceptable; -1: low quality; -2: unacceptable. Those scores were based on the classification of radiologists, a visual classification analysis (Visual Grading Analysis - VGA) was performed according to equation 2.

$$VGA = \frac{\sum Sc_{(0,i)}}{N_i N_0} \quad (2)$$

Where; Sc is the individual score for each observer 0, and the image criteria i, Ni is the total number of image criteria and N0 the total number of observers. Thus, with the classification of radiologists, the VGA calculation was performed, shown in table 2, where each protocol was classified as follows: unacceptable (-2), low quality (-2), acceptable (0), good quality (+1), and great (+2).

Determination of the optimized protocols

According to the subjective criterion, those protocols considered acceptable can be regarded as optimized. Finally, the optimized protocols' dose must be lower than the reference limits of the European protocol^(17, 21-23).

Table 2. Statistical data of the radiographic parameters (kVp and mAs values) and patient anthropometric data for selected X-ray examinations.

Protocol	Subjective spatial resolution	Subjective noise	Visibility of structures	Diagnostic Acceptability	Overall
1	1.9±0.3	1.2±0.4	1.6 ± 0,4	2 ± 0	Optimum
2	1.8 ± 0.4	1±0.4	1.4 ± 0.6	2 ± 0	Optimum
3	1 ± 0	0.4±0.8	0.7 ± 0.4	1.2 ± 0.46	Good Quality
4	0.2 ± 0.4	-0.8±0.8	-0.3 ± 0.4	0.6 ± 0.4	Acceptable
5	0 ± 0.7	-1±0.4	-2 ± 0	-2 ± 0	Unacceptable
6	-2 ± 0	-1±0.4	-1 ± 0.7	-2 ± 0	Unacceptable

+2: Optimum; +1: good quality; 0: acceptable; -1: low quality; -2: unacceptable.

To be able to transfer the optimized techniques to other CT equipment creating a standard image quality model, objective parameters were tested.

Statistical analysis

Statistical analyses focused on calculating means and medians for all objective measurements, covering both dosimetric metrics (CTDIvol, DLP, and SSDE) and image quality parameters (including spatial resolution, CNR, and noise levels). Assessment of differences between protocols was conducted using the Tukey test, indicating the performance of analysis of variance (ANOVA) for group comparisons. Data were described as following a normal distribution after a Shapiro-Wilk test. A significance level of $p<0.05$ was adopted to determine statistical significance in all analyses.

Furthermore, image quality was subjectively evaluated by experienced radiologists using VGA, with results quantified and integrated into additional statistical analyses, although specific methods for this integration were not detailed.

RESULTS

The optimization of computed tomography protocols is detailed in Tables 3 and 4, with evaluations conducted at both 100 kV and 120 kV. Dosimetric assessments, including CTDI, DLP, and SSDE, were performed for each protocol in accordance with European Guidelines, ensuring dose levels remained below reference values. SSDE, reflecting patient dose distribution, was calculated by multiplying CTDIvol⁽²⁴⁾ by a correction factor, with an average LAT of 123.2 mm and anteroposterior distance of 99 mm for all patients⁽²⁵⁾.

Protocols 1 and 2 were rated as optimal, while Protocols 3 and 4 were deemed good and acceptable, respectively. Protocols 5 and 6 were considered unacceptable based on subjective analysis. All protocols-maintained dose quantities below reference levels. Objective parameters of image quality, specifically MTF, were also assessed using an analytical phantom. Notably, in the analysis of spatial resolution (phantom section A), MTF at 40% was scrutinized, as depicted in figure 3.

Regarding the objective parameters of image quality, the first parameter analyzed was MTF. The results of the analysis with the analytical phantom were described below. In phantom section A of spatial resolution, MTF at 40% was analyzed, as shown in figure 3.

For 120 kV, protocols 1, 2, 3 and 4 demonstrated the best spatial resolution. Protocol 1 showed the highest spatial resolution (8.67 cycles.cm⁻¹) followed by protocols 2 and 3 (8.2 and 7.5 cycles.cm⁻¹) and protocol 4 (6.18 cycles.cm⁻¹). Protocols 5 and 6 showed the lowest spatial frequencies at 40% of MTF (5.76 and 5.95 cycles.cm⁻¹). For 100 kV, protocols 1, 2, 3 and 4 demonstrated the best spatial resolution. Protocol 1 showed the highest spatial resolution (8.80 cycles.cm⁻¹), followed by protocols 2 and 3 (8.40 and 7.68 cycles.cm⁻¹) and protocol 4 (6.36

cycles.cm⁻¹). Protocols 5 and 6 showed the lowest spatial frequencies at 40% of MTF (5.25 and 4.94 cycles.cm⁻¹).

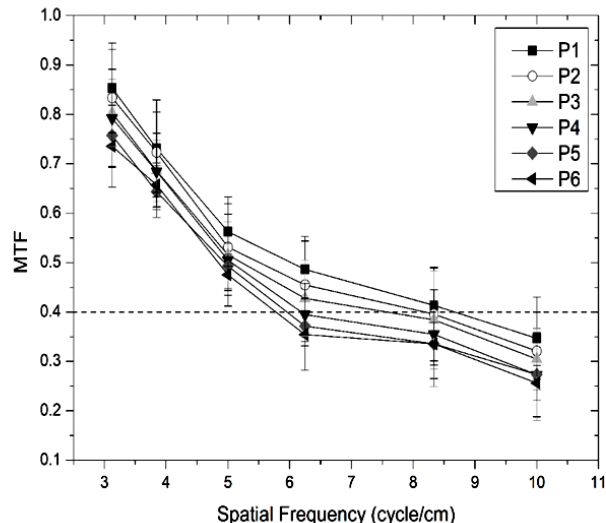


Figure 3. Modulation transfer function (MTF) as a function of spatial frequency (cycles/cm) for six tested protocols. The dashed line shows MTF at 40%.

Thus, this study was able to determine objective quality levels related to the subjective level, e.g., correlating the VGA values, presented in Table 2, with figure 3, the protocols evaluated by radiologists presented diagnostic levels in accordance with the 40% MTF resolution. Protocols 1 and 2 were classified as optimum, with a spatial resolution greater than 8 cycles.cm⁻¹. Moreover, the good quality protocol 3 had a resolution of 7.5 cycles.cm⁻¹, while the protocol of acceptable quality, protocol 4, presented a spatial resolution of 6.8 cycles.cm⁻¹. In addition, the protocols that showed unacceptable diagnostic quality had a spatial resolution of less than 6 cycles.cm⁻¹ than the other ones. The same result was found by relating the objective parameters CNR and noise with the subjective analysis. CNR had a maximum value of 0.72 and a minimum value of 0.24, with values of 0.36 and 0.24, being associated with protocols considered unacceptable. For noise, there was a variation between 5.87 for protocol 1 and 10.38 for protocol 6. Noise level of 8.08 and 10.38 were associated with unacceptable protocols.

Therefore, the diagnostic quality was related to spatial resolution, showing that low dose indices did not present satisfactory spatial resolutions, decreasing the diagnostic efficiency. Conclusions were related directly to the level of SDs assigned to each protocol: low noise levels were related not only to high doses, but also to the high resolution. In the optimization process, all protocols were analyzed according to the following two criteria: subjective analysis of image quality and objective analysis of dose levels. Therefore, the protocols that will be optimized will be those that have been approved by both criteria: low dose and subjective analysis. Thus, protocol 4 presented results consistent with the

optimization criteria, once it presented relevant results to the clinical routine, as described in tables 3 and 4.

In table 3, comprehensive analyses, including objective, subjective, and dosimetric evaluations for the six protocols assessed at 100 kV, were presented. The noise level increased proportionally with higher SD values, resulting in decreased modulation transfer

function (MTF40%) and contrast-to-noise ratio (CNR), while dose levels decreased. Protocol 6 exhibited the lowest CTDIvol, DLP, and SSDE values but had the highest noise level, lowest MTF40%, and CNR, rendering it unacceptable. The Protocols 1 and 2 were classified as the optimum in overall subjective and objective analyses, while Protocols 5 and 6 were classified as unacceptable.

Table 3. Results of objective, subjective and dosimetric analyses with kV 100.

Protocol	1	2	3	4*	5	6
SD	7.5	8.75	10	11.5	12	15
kV	100	100	100	100	100	100
Noise level (HU)	5.23 ± 0.76	6.22 ± 0.74	8.58 ± 0.75	8.82 ± 0.90	9.73 ± 0.36	11.82 ± 0.78
MTF 40%	8.80	8.40	7.68	6.36	5.25	4.94
CNR	15.36 ± 0.84	15.32 ± 1.09	14.41 ± 1.91	11.47 ± 1.14	10.32 ± 1.24	9.74 ± 0.87
CTDI _{vol}	18.50 ± 1.32	16.40 ± 2.15	15.70 ± 1.22	14.30 ± 1.33	12.70 ± 2.40	7.0 ± 3.22
DLP	627.56 ± 12.36	600.25 ± 10.44	513.80 ± 12.96	402.13 ± 16.65	369.25 ± 7.77	254.69 ± 13.88
SSDE	47.23 ± 0.58	42.52 ± 0.99	36.84 ± 0.68	32.49 ± 0.56	25.24 ± 0.69	18.45 ± 0.33
Tube current time (mAs)	145.42 ± 59.84	144.5 ± 47.47	129.52 ± 41.68	128.76 ± 55.34	127.44 ± 29.75	118.92 ± 55.72
Effective dose (mSv)	10.66	10.20	8.73	6.83	6.27	4.32
Overall	Optimum	Optimum	Good Quality	Acceptable	Unacceptable	Unacceptable

SD: Standard Deviation; kV: Kilovolt; MTF: modulation transfer function; CNR: contrast-noise ratio; HU: Hounsfield unit. SSDE: size-specific dose estimate; DLP: dose-length product; CTDIvol: volume computed tomography dose index *Protocol 4 with objective image quality analysis within reference levels, subjective analysis score as "acceptable" and lower radiation dose levels compared to protocols already used in clinical routine.

Table 4. Results of objective, subjective and dosimetric analyses with kV 120.

Protocol	1	2	3	4*	5	6
SD	7.5	8.75	10	11.5	12	15
kV	120	120	120	120	120	120
Noise level (HU)	5.13 ± 0.50	5.27 ± 0.61	5.93 ± 0.54	7.08 ± 0.85	11.27 ± 1.26	13.12 ± 1.38
MTF 40% (cycles.cm ⁻¹)	8.67	8.20	7.50	6.18	5.76	5.95
CNR	21.37 ± 1.30	20.57 ± 1.62	18.99 ± 1.89	16.95 ± 0.74	14.42 ± 1.37	13.82 ± 1.15
CTDI _{vol}	18.2 ± 1.66	14.2 ± 2.13	10.2 ± 2.64	6.9 ± 1.96	5.4 ± 1.33	4.9 ± 1.22
DLP	646.13 ± 15.14	535.2 ± 17.37	418.6 ± 14.97	310.5 ± 14.44	226.4 ± 4.50	145.5 ± 13.20
SSDE	43.61 ± 0.38	36.71 ± 0.88	27.88 ± 0.57	21.94 ± 0.49	16.34 ± 0.33	14.13 ± 0.19
Tube current time (mAs)	107.63 ± 51.03	106.86 ± 51.74	106.63 ± 50.49	106.62 ± 51.50	82.28 ± 35.48	81.42 ± 43.01
Effective dose (mSv)	10.98	9.09	7.11	5.27	3.84	2.47
Overall	Optimum	Optimum	Good Quality	Acceptable	Unacceptable	Unacceptable

SD: Standard Deviation; kV: Kilovolt; MTF: modulation transfer function; CNR: contrast-noise ratio; HU: Hounsfield unit. SSDE: size-specific dose estimate; DLP: dose-length product; CTDIvol: volume computed tomography dose index *Protocol 4 with objective image quality analysis within reference levels, subjective analysis score as "acceptable" and lower radiation dose levels compared to protocols already used in clinical routine.

Similarly, in table 4, detailed analyses for chest CT protocols at 120 kV were provided. Protocols 1 and 2 were identified as optimal based on both radiologists' subjective evaluations and objective parameters. Protocol 3 was rated as acceptable, while protocols 4, 5, and 6 were deemed unsuitable due to inadequate spatial resolution and high noise levels. Importantly, all protocols-maintained dose estimations below reference levels, adhering to the ALARA principle.

DISCUSSION

The present study developed a methodology to optimize chest CT protocols, integrating subjective image quality analyses with objective dose level analyses. This multidimensional approach allowed the creation of a standard image quality model that can be adapted for different CT equipment, highlighting the importance of ATCM variation in the relationship between image quality and radiation

dose.

The utilization of SSDE as a more accurate dose index reflects an advancement in radiation protection, considering patient-specific dimensions. His method aligns with the proposal by Anam *et al.* (21) which emphasized the importance of patient dose assessment based on automated measurements and size-specific dose estimates, finding SSDE values comparable to those observed in our protocol 4. This agreement reinforces the validity of SSDE as a tool in CT protocol optimization.

When comparing our dose analysis results with reference levels (17) and the findings of Soderberg *et al.* (26) consistency in DLP values is observed, suggesting that ATCM-based optimizations can maintain doses within acceptable limits without compromising image quality. This is crucial to ensure patient safety while maintaining diagnostic efficacy.

The application of VGA proved to be an effective technique for quantitative assessment of subjective image quality, corroborating previous studies (27).

The distinction between acceptable and unacceptable protocols, as determined by VGA, reflects a significant correlation with objective quality levels, reaffirming the relevance of an integrated approach in CT protocol optimization.

Regarding the objection the objective analysis of image quality, MTF was essential for assessing the system's ability to represent small objects, a key factor in detecting small nodules and cancer screening⁽¹⁹⁾.

Sookpeng *et al.*⁽¹¹⁾ into the relationship between different noise indices and adaptive statistical iterative reconstruction revealed similar patterns in our MTF analyses, indicating that the use of ATCM may not significantly affect spatial resolution.

The study by Ahmadifard *et al.* supports the use of SSDE as a precise tool for dose assessment in CT examinations. Their research demonstrated that considering patient-specific factors like effective diameter can optimize doses effectively. This aligns with our approach, integrating SSDE with traditional metrics like CTDIvol and DLP to refine protocol optimization for safer yet diagnostically effective doses. Ahmadifard *et al.* found lower than national DRLs for certain scans, highlighting the potential for dose management to reduce patient exposure. Their calculated conversion factors further emphasize the value of SSDE in routine clinical practice, reinforcing our multidimensional approach to CT protocol optimization⁽²⁸⁾.

Additionally, our CNR and noise level analyses emphasize the importance of these parameters in image quality. Protocols with higher SD showed greater noise in the image, which may compromise the detection of low-contrast structures⁽²⁹⁾. The strong inverse correlation between CNR and noise (-0.93) highlights the interdependence of these factors in visualizing objects within the Region of Interest (ROI). As expected, protocols with higher SD presented higher image noise⁽³⁰⁾. In a broader context, optimizing clinical protocols in CT is vital, especially for developing countries. The methodology proposed in this study offers an applicable and replicable approach for diverse diagnostic centers, establishing minimum image quality limits that can guide optimization across different equipment. However, it is important to consider that variations in ATCM parameters between manufacturers may require adjustments in the optimization process.

CONCLUSION

This study assessed six chest computed tomography protocols to optimize radiation doses while maintaining image quality. Protocol 4 emerged as the most effective, meeting quality standards with lower radiation exposure. This approach, guided by the ALARA principle, ensures minimal radiation doses without compromising diagnostic accuracy.

The developed methodology offers broader application in clinical settings utilizing CT scanners.

Conflicts of interest: The authors declare no conflict of interest. The funders had no role in the design of the study; in the collection, analyses, or interpretation of data; in the writing of the manuscript, or in the decision to publish the results.

Data availability statement: The data that support the findings of this study are available on request from the corresponding author. The data are not publicly available due to privacy or ethical restrictions

Committee ethics: The local institutional ethics committee approved this study under our country's regulations.

Funding: This research was funded by São Paulo Research Foundation (Process number: 2020/05539-9) and by Brazilian National Council for Scientific and Technological Development (Process number: 303509/2019-8).

Authors' contribution: All authors were involved in the study and preparation of manuscript equally. All authors approved final version of the manuscript for publication.

REFERENCES

1. Saeed MK, Tammam N, Sulieman A (2021) Assessment of dose reduction and influence of gantry rotation time in CT abdomen examinations. *Int J Radiat Res*, **19**(1): 223-230. doi: 10.29252/ijrr.19.1.223.
2. Bastos Maués NHP, Alves AFF, Pavan ALM, Ribeiro SM, Yamashita S, Trindade AP, *et al.* (2019) Abdomen-pelvis computed tomography protocol optimization: an image quality and dose assessment. *Radiat Prot Dosimetry*, **184**(1): 66-72. doi: 10.1093/rpd/ncy181.
3. Brenner DJ (2014) What we know and what we don't know about cancer risks associated with radiation doses from radiological imaging. *Br J Radiol*, **87**(1035): 20130629. doi: 10.1259/bjr.20130629.
4. Linton OW and Mettler FA (2003) National Council on Radiation Protection and Measurements; National conference on dose reduction in CT, with an emphasis on pediatric patients. *Am J Roentgenol*, **181**(2): 321-329. doi: 10.2214/ajr.181.2.1810321.
5. de González AB and Darby S (2004) Risk of cancer from diagnostic X-rays: estimates for the UK and 14 other countries. *Lancet Lond Engl*, **363**(9406): 345-351. doi: 10.1016/S0140-6736(04)15433-0.
6. Lee D, Choi S, Lee H, Kim D, Choi S, Kim H-J (2017) Quantitative evaluation of anatomical noise in chest digital tomosynthesis, digital radiography, and computed tomography. *J Instrum*, **12**(04): T04006. doi: 10.1088/1748-0221/12/04/T04006.
7. Report No. 184 – Medical Radiation Exposure of Patients in the United States (2019) - NCRP | Bethesda, MD'. Accessed: Apr. 08, 2024. [Online]. Available: <https://ncrponline.org/shop/reports/report-no-184-medical-radiation-exposure-of-patients-in-the-united-states-2019/>
8. Lee S, Yoon SW, Yoo SM, Ji YG, Kim KA, Kim SH, *et al.* (2011) Comparison of image quality and radiation dose between combined automatic tube current modulation and fixed tube current technique in CT of abdomen and pelvis. *Acta Radiol Stockh* **1987**, **52**(10): 1101-1106. doi: 10.1258/ar.2011.100295.
9. Kalra MK, Maher MM, Toth TL, Schmidt B, Westerman BL, Morgan HT, *et al.* (2004) Techniques and applications of automatic tube current modulation for CT. *Radiology*, **233**(3): 649-657. doi: 10.1148/radiol.2333031150.
10. Prasad KN, Cole WC, Haase GM (2004) Radiation protection in humans: extending the concept of as low as reasonably

achievable (ALARA) from dose to biological damage. *Br J Radiol*, **77**(914): 97-99. doi: 10.1259/bjr/88081058.

11. Sookpeng S, Martin CJ, Gentle DJ (2016) Influence of CT automatic tube current modulation on uncertainty in effective dose. *Radiat Prot Dosimetry*, **168**(1): 46-54. doi: 10.1093/rpd/ncu374.
12. Soares FAP, Pereira AG, de Flôr RC (2011) Utilização de vestimentas de proteção radiológica para redução de dose absorvida: uma revisão integrativa da literatura. *Radiol Bras*, 2011 Mar/Abr; **(44)**: 97-103.
13. Nambu A, Sawada E, Kato S, Araki T, Aikawa Y, Yuge M, et al. (2011) Determination of a standard deviation that could minimize radiation exposure in an automatic exposure control for pulmonary thin-section computed tomography. *Jpn J Radiol*, **29** (6): 405-412. doi: 10.1007/s11604-011-0571-0.
14. Diwakar M and Kumar M (2018) A review on CT image noise and its denoising. *Biomed. Signal Process Control*, **42**: 73-88. doi: 10.1016/j.bspc.2018.01.010.
15. Park HJ, Jung SE, Lee YJ, Cho WI, Do KH, Kim SH, et al. (2009) The relationship between subjective and objective parameters in CT phantom image evaluation. *Korean J Radiol*, **10**(5): 490-495. doi: 10.3348/kjr.2009.10.5.490.
16. Miller DL, Balter S, Schueler BA, Wagner LK, Strauss KJ, Vañó E (2010) Clinical radiation management for fluoroscopically guided interventional procedures. *Radiology*, **257**(2): 321-332. doi: 10.1148/radiol.10091269.
17. Doktor K, Vilholm ML, Hardardóttir A, Christensen HW, Lauritsen J (2019) European guidelines on quality criteria for diagnostic radiographic images of the lumbar spine - an intra- and inter-observer reproducibility study. *Chiropr Man Ther*, **27**:20. doi: 10.1186/s12998-019-0241-3.
18. Droege RT and Morin RL (1982) A practical method to measure the MTF of CT scanners. *Med Phys*, **9**(5): 758-760. doi: 10.1118/1.595124.
19. Liu RR, Prado K, Gillin M (2009) Simplified "on-couch" daily quality assurance procedure for CT simulators. *J Appl Clin Med Phys*, **10** (3): 49-55. doi: 10.1120/jacmp.v10i3.2844.
20. Benesty J, Chen J, Huang Y, Cohen I (2009) Pearson correlation coefficient, in *Noise Reduction in Speech Processing*, Cohen I, Huang Y, Chen J, Benesty J (Eds.), Berlin, Heidelberg: Springer. pp: 1-4. doi: 10.1007/978-3-642-00296-0-5.
21. Anam C, Haryanto F, Widita R, Arif I, Dougherty G, McLean D (2018) Volume computed tomography dose index (CTDlvol) and size-specific dose estimate (SSDE) for tube current modulation (TCM) in CT scanning, *Int J Radiat Res*, **16**(3): 289-297.
22. Seeram E (2018) Computed tomography: A technical review. *Radiol Technol*, **89**(3): 279CT-302CT.
23. Brady SL and Kaufman RA (2012) Investigation of American Association of Physicists in Medicine Report 204 size-specific dose estimates for pediatric CT implementation. *Radiology*, **265**(3): 832-840. doi: 10.1148/radiol.12120131.
24. Brink JA and Morin RL (2012) Size-specific dose estimation for CT: how should it be used and what does it mean? *Radiology*, **265**(3): 666-668. doi: 10.1148/radiol.12121919.
25. Dieckmeyer M, et al. (2023) Computed tomography of the head : A systematic review on acquisition and reconstruction techniques to reduce radiation dose. *Clin. Neuroradiol*, **33**(3): 591-610. doi: 10.1007/s00062-023-01271-5.
26. Söderberg M and Gunnarsson M (2010) Automatic exposure control in computed tomography--an evaluation of systems from different manufacturers. *Acta Radiol Stockh Swed* 1987, **51**(6): 625-634. doi: 10.3109/02841851003698206.
27. De Crop A, Bacher K, Van Hoof T, Smeets PV, Vergauwen M, et al. (2012) Correlation of contrast-detail analysis and clinical image quality assessment in chest radiography with a human cadaver study. *Radiology*, **262**(1): 298-304. doi: 10.1148/radiol.11110447.
28. Ahmadifard M, Bakhshandeh M, Mohammadbeigi A, Khoshgard K (2022) Radiation dose of head and abdomen-pelvis computed tomography examinations using size-specific dose estimate. *Int J Radiat Res*, **20**(1): 185-189. doi: 10.52547/ijrr.20.1.28.
29. Brisse HJ, Brenot J, Pierrat N, Gaboriaud G, Savignoni A, De Rycke Y, et al. (2009) The relevance of image quality indices for dose optimization in abdominal multi-detector row CT in children: experimental assessment with pediatric phantoms. *Phys Med Biol*, **54**(7): 1871-1892. doi: 10.1088/0031-9155/54/7/002.
30. Kubo T, Lin PJP, Stiller W, Takahashi M, Kauczor HU, Ohno Y, et al. (2008) Radiation dose reduction in chest CT: a review. *Am J Roent*, **190**(2): 335-343. doi: 10.2214/AJR.07.2556.

